"STATIC AND DYNAMIC ANALYSIS OF HIGH CONTACT RATIO SPUR GEAR DRIVE"

A thesis submitted in the partial fulfillment

of the requirements for the degree of

Master of Technology

In

Mechanical Engineering

[Machine Design and Analysis]

Submitted by

Sonawane Ishan R.

(211ME1162)

Under the esteemed guidance of

Prof. S. C. Mohanty

DEPARTMENT OF MECHANICAL ENGINEERING

NATIONAL INSTITUTE OF TECHNOLOGY ROURKELA

YEAR 2012-2013

NATIONAL INSTITUTE OF TECHNOLOGY

ROURKELA

CERTIFICATE

This is to certify that the thesis entitled, "**STATIC AND DYNAMIC ANALYSIS OF HIGH CONTACT RATI0 SPUR GEAR DRIVE**" submitted by **Mr. Sonawane Ishan R**. in partial fulfillment of the requirements for the award of Master **Of Technology** degree in **Mechanical Engineering** with specialization in **Machine Design and Analysis** at the National Institute of Technology, Rourkela (India) is an authentic work carried out by him under my supervision and guidance.

To the best of my knowledge, the matter embodied in the thesis has not been submitted to any other University / Institute for the award of any degree or diploma.

Date:

Dr. S. C. Mohanty
Assoc. Professor
Department of Mechanical Engineering
National Institute of Technology
Rourkela-769008

ACKNOWLEDGEMENT

First and foremost I offer my sincerest gratitude and respect to my supervisor and guide **Dr. S. C. Mohanty**, Department of Mechanical Engineering, for his invaluable guidance and suggestions to me during my study. I consider myself extremely fortunate to have had the opportunity of associating myself with him for one year. This thesis was made possible by his patience and persistence.

After the completion of this Thesis, I experience a feeling of achievement and satisfaction. Looking into the past I realize how impossible it was for me to succeed on my own. I wish to express my deep gratitude to all those who extended their helping hands towards me in various ways during my tenure at NIT Rourkela. I greatly appreciate & convey my heartfelt thanks to my colleagues, dear ones & all those who helped me in the completion of this work.

I am especially indebted to my parents for their love, sacrifice, and support. They are my first teachers after I came to this world and have set great examples for me about how to live, study and work.

I also express my sincere gratitude to Dr. K. P. Maity, Head of the Department; Mechanical Engineering for valuable departmental facilities.

Sonawane Ishan R.
Roll No: - 211ME1162

INDEX

CHAPTER NO.		TITLE	PAGE NO

LIST OF FIGURES

LIST OF TABLE

ABSTRACT

In this work, an analytical method has been presented for calculating the load sharing among the meshing teeth in high contact ratio spur gearing. Assumption for this procedure is that the tooth deflection at each of two or three pairs of contact is equal in all cases and the sum of normal loads contributed by each of two or three pairs of contact is equal to maximum normal load.

Dynamic loads on high contact ratio spur gears are calculated by using an analytical model based on torsional vibration of gears. Dynamic load variations during a mesh cycle of a tooth are determined. Variable stiffnesses of gear teeth which are required for dynamic load calculations are found by using analytical expressions. Bending, shear, axial compression and Hertzian contact deflections are considered for tooth stiffness calculation. Viscous damping and friction among the mating teeth are also included in this analysis. Contact stresses are calculated by using analytical expressions developed for two elastic bodies held in contact by forces normal to the area of contact and accompanied by tangential frictional force. Contact stress variations during a mesh cycle of a tooth are determined. It is found that the operating speed has a significant influence on the dynamic load acting on the gear tooth. The magnitude and location of maximum dynamic load changes with operating speed.

Keywords- High contact ratio, Spur gears, Mesh stiffness, Dynamic load

MOTIVATION OF WORK

The dynamic analysis of the gears has become important part due to the pressing need of high speed and heavy load carrying machinery. In such applications, due to high precision, periodic variation of tooth stiffness is the only cause of noise and vibration. A high contact ratio spur gear pairs reduces the variation of tooth stiffness and thus to reduce vibration and noise. It also improves structural efficiency, reliability and power to weight ratio. High contact ratio gearing (HCRG) applies to gear meshes that have at least two pairs of teeth in contact at all times i.e. contact ratio of 2.0 or more. This helps in sharing of transmitted load. Unlike the low contact ratio spur gear drive, in high contact ratio spur gear drive the number of pairs of teeth in contact varies between two to three. In low contact ratio pair, the gear tooth is designed for critical loading condition, which corresponds to single pair of teeth contact and the load on gear tooth is maximum transmitted load. Since in a high contact ratio gear drives the minimum pairs in contact are more than one, the load sharing between the pairs to be calculated accurately for economical design of gear drive which will be helpful in design of high contact ratio spur gear drive. A high contact ratio gear pair improves load carrying capacity and also decreases tooth root contact stresses.

OBJECTIVES

The objectives of present work are stated below

- To understand the working of high contact ratio gears.
- Finding out the load sharing between gear teeth.
- To calculate stiffness variation with pinion roll angle.
- Finding out the dynamic load variation with respect to operational speed.
- To determine the principal stresses variation with respect to operational speed.

NOMENCLATURE

x_g, x_p	:	Coordinates perpendicular to the pressure line at the centres of the driven and driving gears respectively
y_g, y_p	:	Coordinates in the direction of the pressure line at the centres of the driven and driving gears respectively
Φ_1	:	Angle between tooth centre line and line joining point c_1 with gear centre O_1
θ_1, θ_2	:	Total angular rotations of driving and driven gears, respectively
θ_p θ_g	:	Fluctuating parts of θ_1 and θ_2, respectively
ω_p, ω_g	:	Rotational speeds of driving and driven shafts, respectively
e_g, e_p	:	Geometric eccentricities of driven and driving gears, respectively
t	:	Time
X_{gi}	:	Displacement of tooth profile of gear i along the line of action
X_r	:	Transmission error
b	:	Half band width of contact
c_1, c_2	:	Points of tangency of the common tangent to gears 1 and 2 respectively
h_1	:	Half tooth thickness below the load point
E_i	:	Young's modulus of elasticity of gear i
K_a , K_b , K_s	:	Stiffness of tooth in axial compression, bending and shear respectively
K_e	:	Effective tooth stiffness
K_h	:	Hertzian contact stiffness of the tooth
K_{pi}	:	Stiffness of teeth pair i
L	:	Face width of tooth
L_p	:	Distance between c_1 and c_2 on the line of contact
m	:	Module of gears

P_o	:	Maximum contact pressure
R_{bi}	:	Radius of base circle of gear i
T_o	:	Base circle pitch
Z_i	:	Number of teeth on gear i
α_0	:	Pitch circle pressure angle
θ_{bi}	:	Half of the tooth thickness angle measured on the base circle of gear i
ρ_i	:	Profile radius of curvature of gear i at the point of contact
ν_i	:	Poisson's ratio of gear i
μ	:	Coefficient of friction
ε	:	Contact ratio
C_{gj}	:	Damping coefficient of teeth pair j
F_{dj}	:	Dynamic load on the teeth pair j
F_{st}	:	Steady transmitted load
F_{pj}	:	Elastic force acting on the pair j
F_{fj}	:	Friction force acting on the pair j
G_{pj}	:	Damping force acting on the gear pair j
J_i	:	Polar mass moment of inertia of gear i
T_i	:	Torque acting on gear i
X_{2j-2}	:	Distance of the teeth pair j from $c_2$on the line of contact
X_{2j-1}	:	Distance of the teeth pair j from c_1 on the line of contact
m_i	:	Mass of the gear i
m_e	:	Resultant mass of the gears
σ_{xx}, σ_{yy}, σ_{zz}	:	Normal stresses
σ_1, σ_2	:	Principal stresses
τ_{zx}	:	Shear stress

CHAPTER 1

INTRODUCTION

1.1 HISTORY OF GEARING

Gears are widely used in almost each type of machineries in the industry. Along with bolts, nuts and screws; they are a common element in machines and will be needed frequently by machine designers to realise their designs in almost all fields of mechanical applications. Ever since the first gear was conceived over 3000 years ago, they have become an integral component in all manner of tools and machineries. The earliest gear drives were crude and used rods inserted in one wheel meshing with identical rods mounted axially in an another wheel as shown in Figure 1.1. These toothed wheels were used to transmit circular motion or rotational force from one part of a machine to another. Gears are used in pairs and each gear is usually attached to a rotating shaft.

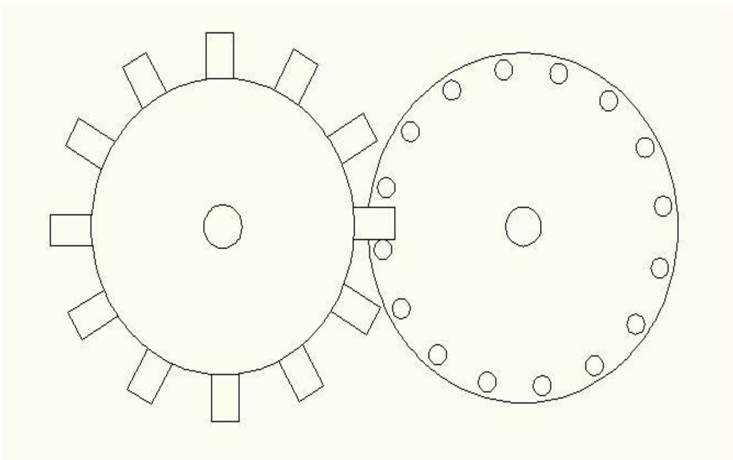

Figure 1.1 Sketch of early gear system

Although ineffective, this type of gear drive performed satisfactorily at low speeds and loads. The main trouble with this system was encountered when the loads and speeds were raised. The contact between the rods were in effect a point contact, giving rise to very high stresses which the materials could not withstand and the use of any lubrication was obsolete due to the contact area, hence high wear was a common occurrence.

Although not so obvious at that time, the understanding of the speed ratio of the gear system was critical. Due to the crude design of the system, the speed ratio was not constant. As a result, when one gear ran at constant speed, there was regular acceleration and deceleration of each tooth of the other gear. The loads generated by the acceleration influence the steady drive loads to cause vibration and ultimately failure of the gear system. Since the 19th century the gear drives designed have mainly been concerned with keeping contact stresses below material limits and improving the smoothness of the drive by keeping velocity ratios as constant as possible. The major rewards of keeping the velocity ratio constant is the reduction of dynamic effects which will give rise to increase in stress, vibration and noise.

Gear design is a highly complicated skill. The constant pressure to build cheaper, quieter running, lighter and more powerful machinery has given rise to steady and advantageous changes in gear designs over the past few decades.

1.2 CONTACT RATIO

Contact ratio is defined as ratio of length of arc of contact to circular pitch. When two gear teeth mesh, the meshing zone is usually limited between the intersecting radii of addendum of the respective gears as shown in Figure 1.2. From the figure it can be seen that the initial tooth contact occurs at point a and final tooth contact occurs at b. If the tooth profiles are drawn through points a and b, they will intersect the pitch circle at points A and B respectively. The radial distance AP is called the arc of approach q_a, and the radial distance PB is called the arc of recess q_r and the sum of these being the arc of action q_t.

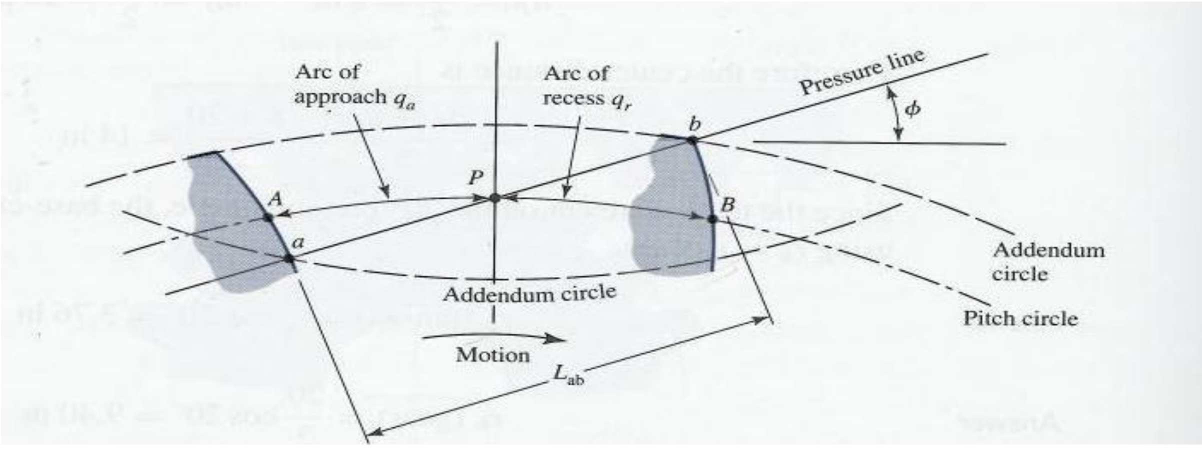

Figure 1.2 Contact ratio

$$q_t = q_a + q_r$$

When the circular pitch p of a mating gear pair is equal to the arc of action q_t, there is always only one pair of teeth in contact, one gear tooth and one pinion tooth in contact and their clearance occupies the space between the arc AB.

$$q_t = p$$

In this case, as the contact is ending at b another tooth simultaneously starts contact at a. In other situations, when the arc of action is greater than the circular pitch, more than one tooth of the gear is always in contact with more than one tooth in the pinion, meaning that as one tooth is ending contact at b, another tooth is already been in contact for a small period of time starting at a. For a short span of time there will be two teeth in contact, one near A and the other near B. As the gear pair rotates through their meshing cycle, the tooth near B will cease to be in contact and only a single pair of contacting teeth will remain, and this process repeats itself over the period of operation. The contact ratio provides the average number of teeth pairs in contact.

Most gears are generally designed with a contact ratio of more than 1.2, as the contact ratio is generally reduced due to errors in mounting and assembly of the gear pairs. Gear pairs operating with low contact ratio are susceptible to interference and damage as a result of impacts between teeth and thereby leading to an increased level of noise and vibration.

Gears are generally designed with contact ratios of 1.2 to 1.6. A contact ratio of 1.6, for example, means that 40 per cent of the time one pair of teeth will be in contact and 60 per cent of the time two pairs of teeth will be in contact. A contact ratio of 1.2 means that 80 per cent of the time one pair of teeth will be in contact and 20 per cent of the time two pairs of teeth will be in contact. Gears with contact ratio greater than 2 are referred to as "high-contact-ratio gears." For these gears there are never less than two pairs of teeth in contact. A contact ratio of 2.2 means that 80 per cent of the time two pairs of teeth will be in contact and 20 per cent of the time three pairs of teeth will be in contact. High contact ratio gears are generally used in selected applications where long life is required. Analysis should be performed when using high contact ratio gearing because higher bending stresses may occur in the tooth addendum region. Also higher sliding in the tooth contact can contribute to distress of the tooth surfaces. In addition higher dynamic loading may occur with high contact ratio gearing.

1.3 HIGH CONTACT RATIO GEARS

Contact ratio is defined as the average number of pairs of teeth in contact under static conditions, and with no errors and tooth profile modifications. The term high contact ratio (HCR) means the gearing that has at least two pairs of teeth in contact at all times i.e. contact ratio is 2 or more. The percentage change in mesh stiffness for HCR meshes is lower than low contact ratio (LCR) meshes, so high-quality HCR gear meshes have lower mesh induced vibration and noise than LCR gear meshes.

In advanced gear transmission design, main goals are increased life and reliability and reduced weight of a gear. High contact ratio gears (HCRG) provides an effective means for achieving these goals. In HCRG, at least two pairs of teeth in contact at all times, whereas in standard low contact ratio gears (LCRG), alternate between one and two pairs are in contact. This enables higher power-to-weight ratio longer life and greater reliability because the transmitted load is shared between two or more pairs of teeth; the individual tooth load and stress are less for HCRG than for LCRG designs. HCRG are expected to be dynamically more sensitive to tooth profile. In gear performance, dynamic loads and stresses are important. High dynamic loads will increase gear noise and the risk of surface failure, and large value of dynamic stress at the tooth root can lead to premature tooth fatigue and fracture. Dynamic analysis is required to determine the load sharing between the two and three pairs in contact.

CHAPTER 2

LIETURATURE STUDY

2.1 LITERATURE STUDY

Tuplin (1950) [1] suggested that the number of stress cycles causing failure of a given material under any particular stress is dependent of the time-rate of repetition of stress. High-speed gears have failed under stresses lower than the fatigue limit so it becomes necessary to consider whether the actual stress was as low as had been assumed. Pitch errors and profile variation in gear teeth cause actual stresses to be higher than nominal stresses. The nominal permissible stress (corresponding to the mean transmitted torque) should therefore consider probable errors in the teeth. So spring mass model of mating gears is developed. Equivalent stiffness was calculated by considering individual stiffnesses. Dynamic loads were approximated by considering various types of errors.

Houser et al. (1970)[3] investigated dynamic factors for spur and helical gears. Comprehensive program was developed for spur and helical to investigate the influence of errors and variation in mesh stiffnesses on peak stresses. Four sets of specially designed gears were tested. Tooth loads and system shaft torques at various operating conditions were compared.

Wilcox et al. (1973) [4] explained the analytical method of finite elements for analysis of gear tooth stresses. Necessary details for simulating a two-dimensional tooth shape with finite elements were outlined and stress values at the tooth surface in the root fillet were determined. Tensile fillet stress in generated tooth shapes considering either symmetric or asymmetric profiles was analysed using finite element analysis. Stress data obtained were used to develop a new simplified stress formula which gives tensile fillet stress as a function of geometric tooth shape and general loading conditions.

Staph (1976) [5] developed a computer program to design external spur gears having normal contact ratios (<2) and high contact ratios (≥ 2). Effects of changes in gear parameters on several performance factors of high contact ratio gears were studied. Then results were compared with those for the equivalent normal contact ratio gears. It was concluded that a high contact ratio gear obtained by increasing the addendum of an equivalent normal contact ratio gear have lower bending and compressive stresses (favourable) and increased friction heat generation and flash temperatures (unfavourable).

Cornell et al. (1978) [6] presented a solution for a dynamic model of spur gear systems for all practical contact ratios. The dynamic response of the gear system and the associated tooth loads and stressing were determined in this analysis. The dynamic model considered the two gears as a rigid inertia and the teeth act a variable spring of a dynamic system which was excited by the meshing action of the teeth. The effects of different parameters like non-linearity of the tooth pair stiffness in meshing, the tooth errors and the tooth profile modifications were included in this study. It concluded that system inertia and damping, tooth profile modification and system critical speeds affect the dynamic gear tooth loads and stressing dominantly.

J.W.Lund (1978) [7] described method for calculating the coupled torsional-lateral vibrations in a geared system of rotors. In this paper both forced vibrations and free damped vibrations whose complex Eigen frequencies define the damped critical speeds and the stability of the rotor system were considered. The Holzer method was used for torsional vibrations and the Myklestad Prohl method was used for lateral vibrations, after which they were coupled through impedance matching at the gear meshes.

Elkohly (1985) [9] gave solution for the calculations of load sharing between teeth in mesh for high contact ratio gears. In this analysis the sum of tooth deflection, spacing error and profile modification was assumed to be equal for all pairs in contact. Also the sum of normal loads taken by pairs was assumed to be equal to the maximum normal load. Stiffness variation along path of contact was considered. Tooth fillet stress, contact stress were determined using tooth geometry after individual load were calculated. The results obtained from experimental analysis were compared with analytical results.

Ozguven et al. (1988) [11] used single degree of freedom non-linear model for the dynamic analysis of gear pair. Calculations for the dynamic mesh and tooth forces, dynamic factors based on stresses and dynamic transmission error from measured or calculated loaded static transmission errors were performed by two methods and a computer program was developed. The effects of variable mesh stiffness and damping, gear errors pitch, profile errors, run out errors, profile modifications and backlash were also discussed in this analysis. One of the methods was accurate and the other one was approximate. In the first method, the time variation of both mesh stiffness and damping was demonstrated with numerical examples. In the second method, the time average of the mesh stiffness was used. However, the excitation effect of the variable mesh stiffness was included in the formulation used in approximate analysis. It was concluded from the comparison of the results of the two methods that the displacement excitation resulting from variable mesh stiffness was more important than the change in system natural frequency resulting from the mesh stiffness variation.

Kahraman et al. (1991) [12] included coupling between the transverse and torsional motions at the gear in appropriate dynamic model of a spur gear pair. Though various numerical models with large degrees of freedom based on the transfer matrix method or the finite element method were available, reduced order analytical models were preferred for design calculations or for non-linear analysis. In this study they proposed such model and determined the associated error in the undamped Eigen solution by a comparison with a finite element model.

Kahraman et al. (1992) [13] developed a finite-element model for investigation of dynamic behaviour of geared rotor. Transverse vibration of bearing and transverse and torsional vibration of shaft were taken into account for this analysis. In this model the rotary inertia of shaft , the axial loading on shafts, bearing flexibility and damping, material damping of shafts and the stiffness and the damping of gear mesh were included. The coupling between the torsional and transverse vibrations of gears was considered in the model. Mesh stiffness was assumed to be constant. The dynamic mesh forces due to these excitations were calculated.

Ramamurti et al. (1998) [15] presented the findings of three-dimensional stress analysis of spur and bevel gear teeth by Finite element method using cyclic symmetry concept. The displacement of a tooth was computed for each Fourier harmonic component of the contact line load and all the components were added to obtain the total displacement. This displacement was used in the calculation of static stress in the teeth. The sub matrices elimination scheme was used for calculation of natural frequencies and mode shapes. This analysis demonstrated the use of cyclic symmetry concept in the Finite Element Analysis of spur gear. This approach helps in large saving in computer memory and reduction of computational effort. The dynamic analysis of gear tooth was efficiently done by this approach utilising the geometrical periodicity and the sub matrices elimination scheme.

Parker et al. (2000) [16] investigated dynamic response of a spur gear pair using a Finite element/contact mechanics model which suits well for dynamic gear analyses. The gear pair was tested across a wide range of operating speeds and torques. Comparisons were made with other researcher's published experiments that reveal complex non-linear phenomena. The non-linearity in meshing was due to the contact loss of the meshing teeth. It occurs even for large torques for high-precision gears also. Dynamic mesh forces were calculated using a detailed contact analysis at each time step as the gears roll through the mesh. Mesh forces are determined by contact analysis in combination with a unique semi-analytical Finite element formulation at the tooth mesh.

Huang et al. (2000) [17] considered a spur gear tooth as a variable cross-section Timoshenko beam to develop a dynamic model to obtain transient response for spur gears of involute profiles. A dynamic stiffness method using equations of motion of a Timoshenko beam model was developed to simulate spur gear dynamics during meshing. In this study the dynamic responses of a single tooth and a gear pair were investigated. Firstly, Gear blank and tooth profile were represented as polynomials. The dynamic stiffness matrix and natural frequencies of the gear were calculated. The modal analysis was used to calculate the forced response of a tooth subject to a shaft-driven transmission. The forced response was obtained at arbitrary points in a gear tooth. They considered time varying stiffness and mass matrices and the gear meshing forces at moving meshing points during the study.

Kapelevich (2000) [18] developed the basic geometry theory for asymmetric gear teeth. Method of design of spur gears with asymmetric teeth was described so as to increase load carrying capacity, minimize weight, overall dimension and vibration levels. It was concluded that load carrying capacity increases and weight, size decreases with increase in contact ratio and pressure angle for drive sides. Also the formulas and equations for gear and generating rack parameters were determined in this study.

Choi et al. (2001) [19] presented an analytical study of the dynamic characteristics of a geared rotor-bearing system by the transfer matrix method. Rotating shafts of the system were modeled as Timoshenko beams with effects of shear deformation and gyroscopic moment. The gear mesh was modeled as a pair of rigid disks connected by a spring-damper set along the pressure line and the transmission error was simulated by a displacement excitation at the mesh. The transfer matrix of a gear mesh was developed. The coupled lateral-torsional vibration of a geared rotor-bearing system was studied. Natural frequencies and corresponding mode shapes, and whirl frequencies under different spin speeds were determined. In addition, steady-state responses due to the excitation of mass unbalance, transmission error and geometric eccentricity gear mesh are obtained. Effect of the time-varying stiffness of the gear mesh was investigated.

Fong et al. (2002) [20] proposed a mathematical model for parametric tooth profile of spur gear by using a given equation of line of action. The line of action was considered to be usually composed of only simple curves. By combining simple curves into the line of action the proposed mathematical model enhanced the freedom of tooth profile design. The equation of line of action was used to derive curvature, sliding velocity, contact ratio, and the limitation of undercutting. Based on the proposed mathematical model, both mating tooth profiles by the single parameter of line of action were presented. In this work the kinematical characteristics of mating gears with nonstandard tooth profiles were studied.

Vedmar et al. (2003) [21] described method to calculate dynamic gear tooth force and bearing forces. The model developed in this study also includes elastic bearings. Path of contact and gear mesh stiffness were determined using the deformations of the gears and the bearings. This analysis gave contact outside the plane of action and a time varying working pressure angle. The influence of the friction force was also studied. Dynamic influence on the gear contact force or on the bearing force in the gear mesh line-of-action direction was not considered due to friction. On the other hand, the changing of sliding directions in the pitch point was a source for critical oscillations of the bearings in the gear tooth frictional direction. These oscillations in the frictional direction appear unaffected by the dynamic response along the gear mesh line of action direction.

Maliha et al. (2004) [22] described a nonlinear dynamic model for a gear shaft disk bearing system. This model of a spur gear pair was coupled with linear finite element models of shafts on which gears are mounted. The nonlinear elasticity term due to backlash was expressed by a describing function. The excitations considered in the model were external static torque and internal excitation caused by mesh stiffness variation, gear errors and gear tooth profile modifications. This work combines the versatility of modeling a shaft-bearing disk system that can have any configuration without a limitation to the total degree of freedom, with the accuracy of a nonlinear gear mesh interface model that allowed predicting jumps and double solutions in frequency response

Wang et al. (2005) [23] outlined methods for using FEA of high contact ratio spur gears in mesh, considering adaptive meshing and element size selection under the solution accuracy criteria. These methods were proficient in a range of loads over the mesh cycle, with and without modification in tooth profile. This study demonstrated the high contact ratio gears to provide significant advantages for decreasing tooth root and contact stresses and also increased load carrying capacity. Earlier numerical work using FEA was limited due to several factors; (i) the difficulty in predicting load sharing over roll angles covering two or three teeth simultaneously in mesh (ii) the problem of primary unconstrained body motion when (long) profile modifications were applied. Methods and results for overcoming these difficulties with recent computer hardware and software improvements were presented in this study. Particular developments discussed include the use of FE analysis of High Contact Ratio Gears in mesh and the results obtained when adaptive meshing was used.

Shuting Li (2007) [24] presented three-dimensional (3-D), finite element methods (FEM) to conduct surface contact stress (SCS) and root bending stress (RBS) calculations of a pair of spur gears with machining errors (ME), assembly errors (AE) and tooth modifications (TM). In this paper, firstly positions of a pair of parallel-shaft spur gears with ME, AE and TM were defined in a 3-D coordinate system. The tooth contact of the gear pair was assumed on a reference face around the geometrical contact line. Deformation influence coefficients of the pairs of contact points were calculated by 3-D, FEM and loaded tooth contact analysis (LTCA) of the pair of gears with ME, AE and TM was conducted by mathematical programming method. Tooth contact pattern and root stains of a spur gear pair with assembly errors were calculated using the programs and these results were compared with experimental results. Calculated results were in agreement with the measured ones well. It is concluded that surface contact stress and root bending stress were greater than the case without errors and tooth modifications.

Podzharov et al. (2008) [25] used high contact ratio spur gears to exclude or reduce the variation of tooth stiffness. In this work the analysis of static and dynamic transmission error of spur gears with standard tooth of 20° profile angle was presented. A simple method for designing spur gears having a contact ratio nearly 2.0 was used. It included the increasing the number of teeth on mating gears and simultaneously introducing negative profile shift in order to provide the same center distance. A tooth mesh of periodic structure was used to consider deflection and errors of each pair of teeth in the engagement. Computer programs were developed to calculate static and dynamic transmission error of gears under load. This analysis of gears concluded that gears with high contact ratio have much less static and dynamic transmission error than standard gears.

Shuting Li (2008) [26] investigated the effect of addendum on tooth contact strength, bending strength and other performance parameters of spur gears. Mathematical programming method (MPM) and finite element method (FEM) were used together to conduct loaded tooth contact analyses (LTCA), deformation and stress calculations of spur gears with different addendums and contact ratios. Tooth load, load-sharing, contact stresses, root bending stresses, transmission errors and mesh stiffnesses of the spur gears were analyzed. Effects of addendum and contact ratio on gear strength and basic performance parameters were also discussed.Finally, strength calculations of HCRG by considering misalignment error and lead crowning were presented in this paper.

Karpat et al. (2008) [27] presented paper in which the primary objective was to use dynamic analysis to compare conventional spur gears with symmetric teeth and spur gears with asymmetric teeth. The secondary objective was to optimize the asymmetric tooth design in order to minimize dynamic loads. This study described preliminary results to designers for understanding dynamic behaviour of spur gears with asymmetric teeth. A dynamic model was developed during study, using MATLAB, and used for the prediction of the instantaneous dynamic loads of spur gears with symmetric and asymmetric teeth. For asymmetric teeth, the dynamic factor decreases with increase in addendum. Also the static transmission error decreases with increasing pressure angle. It is concluded that the amplitudes of harmonics of the static transmission errors were reduced for asymmetric teeth with long addendum high gear contact ratio gears.

Kim et al. (2010) [28] analysed the dynamic response of a pair of spur gears having translational motion due to bearing deformation. A new dynamic model for the gear set was formed considering translational motion which means the distance between the centres of a pinion and a gear varies with time. So the pressure angle and the contact ratio were considered as time varying variables. The dynamic responses were computed by applying the Newmark time integration method after deriving nonlinear equations of motion for gears. The new model gave more accurate dynamic responses. The effects of damping and stiffness upon the dynamic responses were also investigated.

Ristivojevic et al. (2013) [29] studied the impact of load distribution in meshed teeth. Also teeth geometry and manufacturing accuracy on wear of the spur gear tooth flanks were studied in this paper. Due to wearing causes uneven load distribution hence dynamic forces increases, and thus energy efficiency was decreases. A larger number of impacts on the tooth flanks stress state were taken into account so as to reach more accurate model for the analysis of tooth flanks load carrying capacity. A mathematical model depending on the value and sign of base pitch difference of meshed teeth developed for the contact stress during contact period. It was concluded that the original geometry and proper teeth mesh were impaired by adhesive wear. This results in the lower efficiency, larger variation of load distribution and higher dynamic forces. Uniformity and intensity of tooth flanks wear depend on pitch point position on the profiles of meshed teeth.

Rincon et al. (2013) [30] presented the procedure to determine loaded transmission error of a spur gear transmission as well as meshing stiffness and load sharing ratio. The procedure also allows a better representation of load transfer between teeth pairs. The analysis of contact forces and deformations in spur gear transmissions was done using an advanced model. The deformation at each gear contact point was assumed as a combination of a global and a local term. The global term was obtained by means of a finite element model and the local term was described by an analytical approach derived from Hertzian contact theory. The quasi static behaviour of a single stage spur gear transmission was discussed in this study using numerical example, which showed the capabilities of the methodology to obtain the loaded transmission error under several load levels as well as some other related measures such as load ratio or meshing stiffness.

2.2 PRESENT WORK

The dynamic analysis of the gears has become important part due to the pressing need of high speed and heavy load carrying machinery. A high contact ratio spur gear pair reduces the variation of tooth stiffness and thus to reduce vibration and noise. It also improves structural efficiency, reliability and power to weight ratio. With increased requirements of high speed, heavy load and light weight in gear design, the dynamic load is required to determine among two or three pairs in contact. In this work, an analytical method is discussed for calculation of the load sharing among meshing teeth pairs. Also variations of dynamic load during mesh cycle are determined. Variable stiffnesses which are required for dynamic load calculations are found using analytical expressions.

This information may be useful in further analysis of High Contact Ratio Spur Gear drives.

CHAPTER 3

MATHEMATICAL MODELLING

3.1 EQUATION OF MOTION

A typical geared rotor system is shown in Figure 3.1. It consists of a motor connected to one of the shafts by a coupling, a load at the other end of the other shaft and a gear pair which couples the shafts. Both shafts are supported at several locations by bearings. Hence system consists of following elements.

1) Shafts

2) Rigid disks

3) Flexible bearings

4) Gears

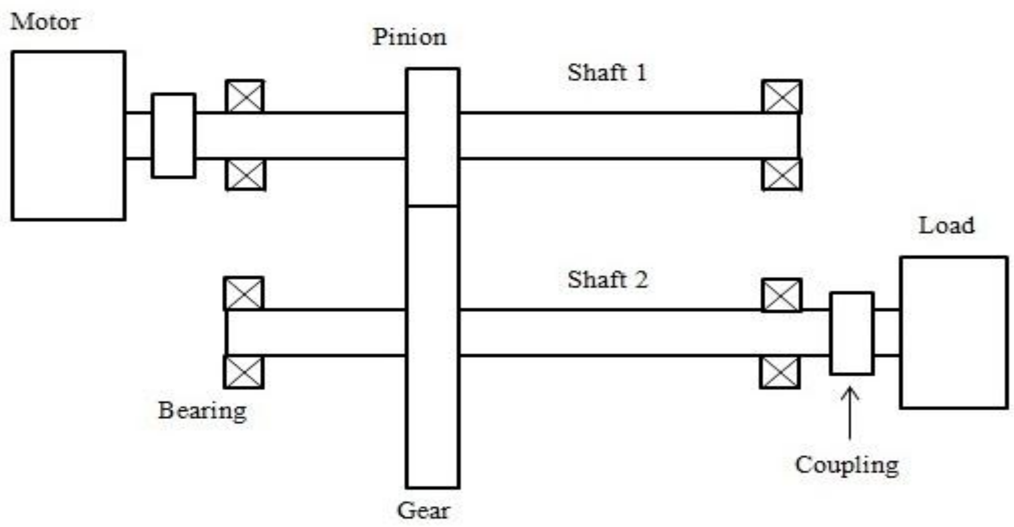

Figure 3.1 Typical gear rotor system

When two shafts are not coupled, each gear can be modelled as a rigid disk. However when they are in mesh, these rigid disks are connected by a spring damper element representing the mesh stiffness and damping.

A typical gear mesh represented by a pair of rigid disks connected by a spring and a damper along the pressure line which is tangent to the base circles of the gears in Figure 3.2.

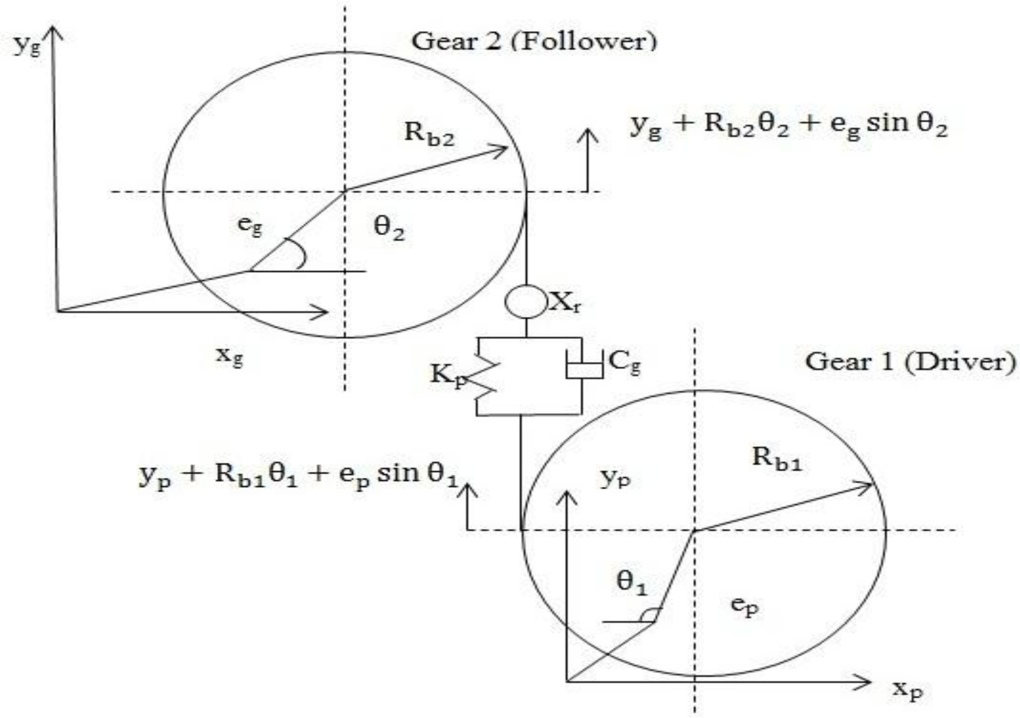

Figure 3.2 Modelling of a gear mesh

X_{gi} is displacement of tooth profile of gear i along the line of action.

$$X_{g1} = y_p + R_{b1}\theta_1 + e_p \sin\theta_1 \quad (1)$$

$$X_{g2} = y_g + R_{b2}\theta_2 + e_g \sin\theta_2 \quad (2)$$

e_p and e_g are geometric eccentricities of driving and driven gears. R_{b1} and R_{b2} are base circle radii of the driving and driven gears. The angles θ_1 and θ_2 are the total angular rotations of the driving and driven gears, respectively, and are equal to

$$\theta_1 = \theta_p + \omega_p t \quad (3)$$

$$\theta_2 = \theta_g + \omega_g t \quad (4)$$

Where θ_p and θ_g are the alternating parts of rotations and ω_p and ω_g are the spin speeds of the driving and driven shafts, respectively. The displacement X_r is considered as the transmission error at mesh point.

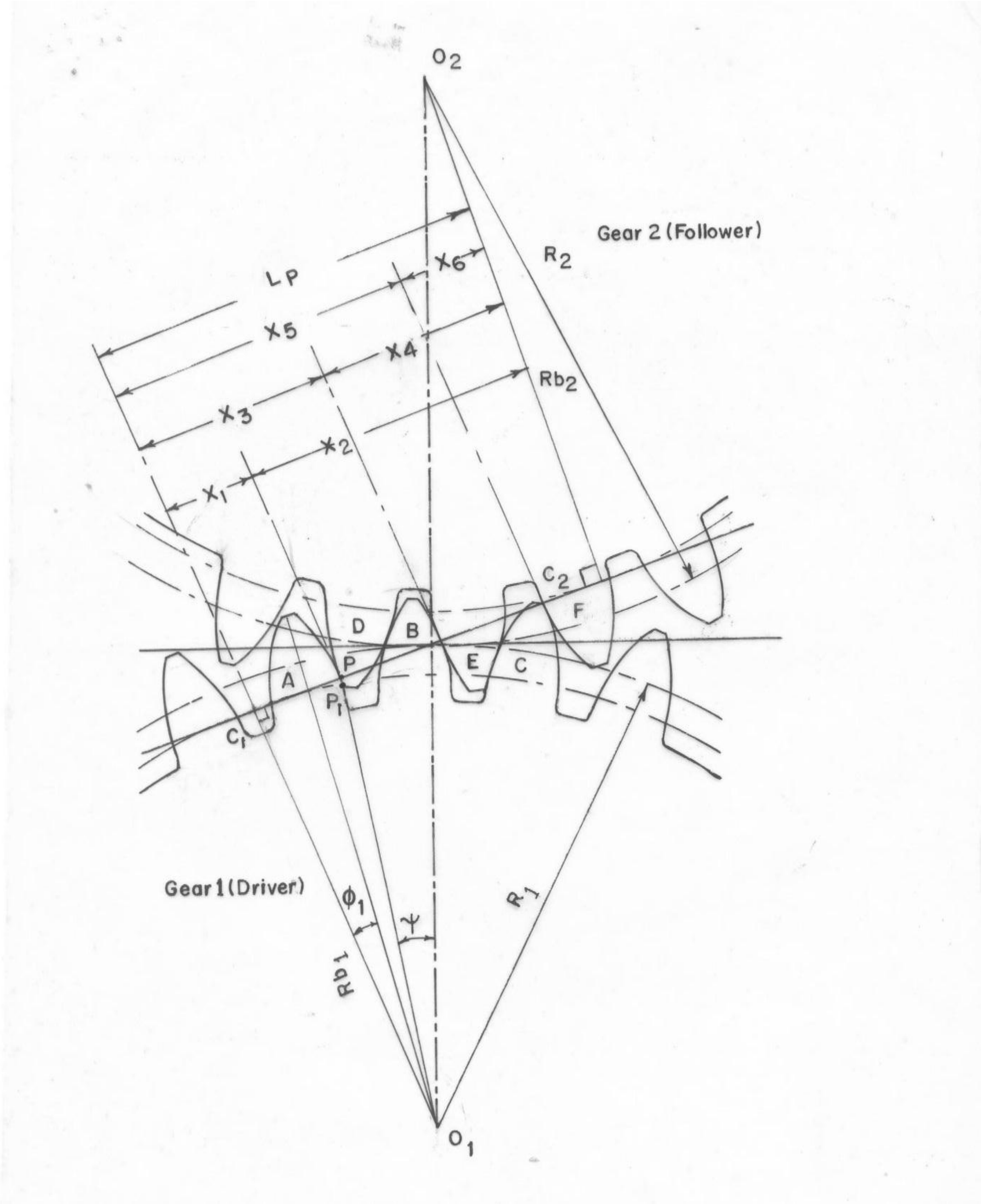

Figure 3.3 Teeth meshing in high contact ratio gears

In this study, the dynamic loads on high contact ratio spur gears are calculated by using an analytical model based on torsional vibration of gears. In the present analysis, the gear and pinion teeth are the only energy storing elements. Elasticity of the other components of the drive has not been taken into account. Equation of motion governing the angular displacements of the pinion and gear including the friction forces between the contacting teeth and a viscous damping force can be derived by using the free body diagrams of each gear which are given in Figure 3.3.

$$J_1\ddot{\theta}_1 = \left[T_1 - \{F_{p1} + G_{p1}\}R_{b1} - F_{f1}X_1 - \{F_{p2} + G_{p2}\}R_{b1} - F_{f2}X_3 - \{F_{p3} + G_{p3}\}R_{b1} - F_{f3}X_5\right] \tag{5}$$

$$J_2\ddot{\theta}_2 = \left[-T_2 + \{F_{p1} + G_{p1}\}R_{b2} + F_{f1}\{L_p - X_1\} + \{F_{p2} + G_{p2}\}R_{b2} + F_{f2}\{L_p - X_3\} + \{F_{p3} + G_{p3}\}R_{b2} + F_{f3}\{L_p - X_5\}\right] \tag{6}$$

Using the relations given below, the equation of motion in terms of transmission error X_r is obtained.

$$m_1 = \frac{J_1}{R_{b1}^2} \tag{7}$$

$$m_2 = \frac{J_2}{R_{b2}^2} \tag{8}$$

$$F_{st} = \frac{T_1}{R_{b1}} = \frac{T_2}{R_{b2}} \tag{9}$$

$$F_{pj} = K_{pj} * X_r \tag{10}$$

$$G_{pj} = C_{gj} * \dot{X}_r \tag{11}$$

$$F_{fj} = \mu * F_{pj} \tag{12}$$

The equation of motion in terms of X_r is given below

$$\ddot{X}_r + [K_{p1}(s_{p1}m_2 + s_{g1}m_1) + K_{p2}(s_{p2}m_2 + s_{g2}m_1) + K_{p3}(s_{p3}m_2 + s_{g3}m_1)] * \frac{X_r}{m_1 m_2} + [C_{g1}(s_{p1}m_2 + s_{g1}m_1) + C_{g2}(s_{p2}m_2 + s_{g2}m_1) + C_{g3}(s_{p3}m_2 + s_{g3}m_1)] * \frac{\dot{X}_r}{m_1 m_2} = F_{st}\left(\frac{m_1 + m_2}{m_1 m_2}\right) \tag{13}$$

$$X_r = X_{g1} - X_{g2} \tag{14}$$

$$\dot{X}_r = \dot{X}_{g1} - \dot{X}_{g2} \tag{15}$$

$$\ddot{X}_r = \ddot{X}_{g1} - \ddot{X}_{g2} \tag{16}$$

$$C_{gj} = 2 * \xi * \sqrt{K_{pj} * m_e} \tag{17}$$

$$m_e = \frac{m_1 m_2}{m_1 + m_2} \tag{18}$$

$$S_{pj} = 1 \pm \frac{X_{2j-1} * \mu}{R_{b1}} \tag{19}$$

$$S_{gj} = 1 \pm \frac{(L_P - X_{2j-1}) * \mu}{R_{b2}} \tag{20}$$

Where j=1, 2 and 3

In the above relations, if the speed of the driver is greater than the speed of follower, the sign is positive otherwise negative.

The coefficient of friction between the contacting teeth is calculated by using the semi empirical formula

$$\mu = 0.05e^{-0.125V_s} + 0.002\sqrt{V_s} \quad (21)$$

Where V_s is the sliding speed measured in m/sec

The damping ratio ξ has a value in the range of 0.03 to 0.17.

In this study, it is taken as 0.1.

3.2 STIFFNESS CALCULATION

The locations and sizes of the two and three pairs of teeth contact zones can be determined from the contact ratio and base pitch of the gear pair. These zones are shown in Figure 3.4.

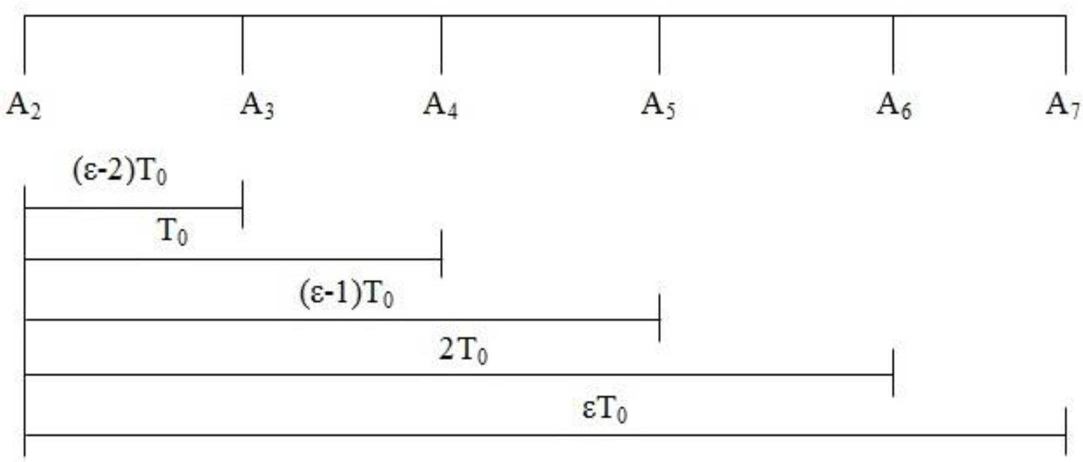

Figure 3.4 Alteration of number of contact pairs

A_2-A_3, A_4-A_5, A_6-A_7 – Three pairs of teeth contact zones

A_3-A_4, A_5-A_6 – Two pairs of teeth contact zones

Different contact lengths are shown in above figure.

After determining the positions and widths of these contact zones, the corresponding pinion or gear roll angles are determined from the gear geometry, since each point on the common normal line can be mapped to a corresponding point on the base circle, using the involute properties of the spur gear tooth.

Referring to the Figure 3.3, ψ is the angle between the line joining gear centres O_1, O_2 and the line O_1P_1, where P_1 is the corresponding point of contact P is mapped on the base circle. The angles ψ for the reference points A_2, A_3, A_4, A_5, A_6 and A_7 representing the locations of two and three pairs of teeth contact zones on the common normal line and they are represented as under.

$$\psi_{a2} = -(\alpha_0 - \beta_{b2}) \tag{22}$$

$$\psi_{a3} = \psi_{a2} + (\epsilon - 2) * 2\pi/z_1 \tag{23}$$

$$\psi_{a4} = \psi_{a2} + 2\pi/z_1 \tag{24}$$

$$\psi_{a5} = \psi_{a2} + (\varepsilon - 1) * 2\pi/z_1 \tag{25}$$

$$\psi_{a6} = \psi_{a2} + 4\pi/z_1 \tag{26}$$

$$\psi_{a7} = \psi_{a2} + \varepsilon * 2\pi/z_1 \tag{27}$$

$$\beta_{b2} = \sqrt{{R_{a1}}^2 - {R_{a2}}^2} - \varepsilon * T_0 \tag{28}$$

The angular displacement of gear 1 measured from the gear centre line O_1O_2 to the symmetric line the gear tooth is

$$\theta_1 = \psi - \theta_{b1} \tag{29}$$

$$\theta_{b1} = \frac{\pi}{2z_1} + \mathrm{inv}(\propto_0) \tag{30}$$

The angle Φ_1 can be related to θ_1 which is again represented as

$$\Phi_1 = \propto_0 + \theta_1 \tag{31}$$

Where Φ_1 is the angle between the symmetrical line of tooth and line O_1 C_1. This is also the inclination angle of load line with the normal to the symmetrical line of the tooth.

3.2.1 TOOTH STIFFNESS

To determine the tooth stiffness bending, shear, axial compression and contact deflections of the gear tooth are considered. The following expressions for these stiffnesses were suggested by Yang and Lin [10] and Nayak [14].

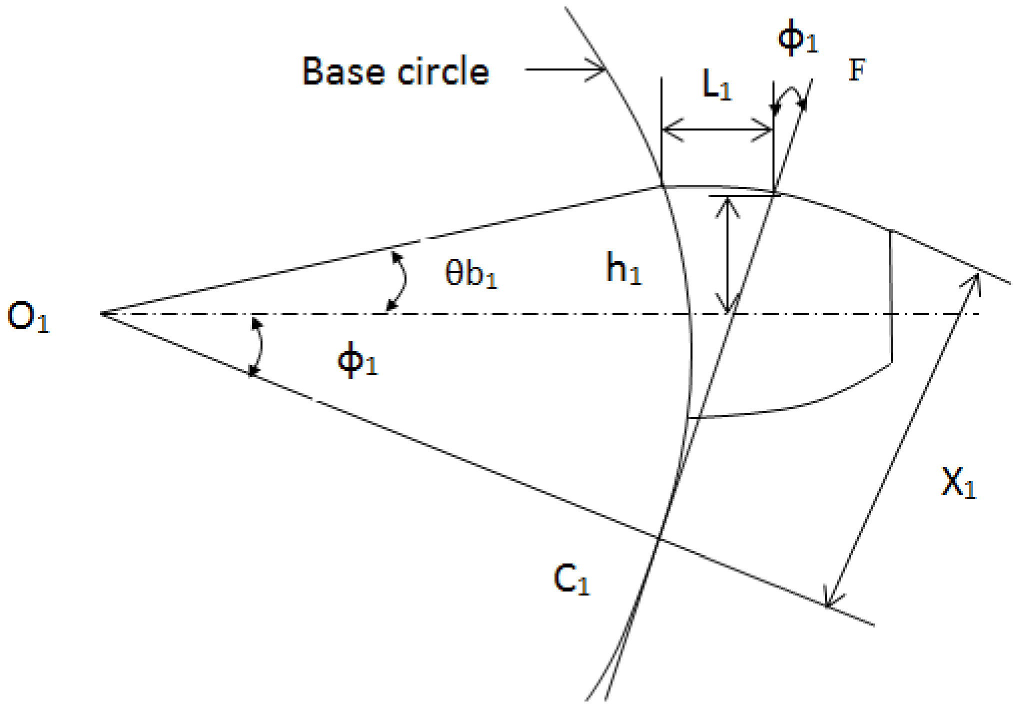

Figure 3.5 Tooth of a gear

Bending stiffness of the gear tooth (K_b)

$$\frac{1}{K_b} = \int_{-\Phi_1}^{\theta_{b1}} \frac{P_b(\tau)}{Q_b(\tau)} d\tau \tag{32}$$

Where

$$P_b(\tau) = 3\left\{\cos\Phi_1\left[\frac{1}{R_{b1}} - \cos\theta_{b1} - \cos\tau + (\theta_{b1}-\tau)\sin\tau\right] - \frac{h_1}{R_{b1}}\sin\Phi_1\right\}^2 [(\theta_{b1} - \tau)\cos\tau] \quad (33)$$

$$Q_b(\tau) = 2E_1L[\sin\tau + (\theta_{b1}-\tau)\cos\tau]^3 \quad (34)$$

Axial compression stiffness (K_a)

$$\frac{1}{K_a} = \int_{-\Phi_1}^{\theta_{b1}} \frac{P_a(\tau)}{Q_a(\tau)} d\tau \quad (35)$$

Where

$$P_a(\tau) = (\theta_{b1}-\tau)(\sin\Phi_1)^2 \quad (36)$$

$$Q_a(\tau) = 2E_1L[\sin\tau + (\theta_{b1}-\tau)\cos\tau] \quad (37)$$

Shear stiffness of the tooth (K_s)

$$\frac{1}{K_s} = \int_{-\Phi_1}^{\theta_{b1}} \frac{P_s(\tau)}{Q_s(\tau)} d\tau \quad (38)$$

Where

$$\begin{aligned} P_s(\tau) = [3(1+\nu_1)(\cos\Phi_1)^2]\Bigg[&2(\theta_{b1}-\tau)\{(\theta_{b1}-\tau)\cos\tau + \sin\tau\} \\ &* \left\{(\theta_{b1}-\tau)(1+(\sin\tau)^2) + \cos\theta_{b1}\sin\tau - \frac{(L_1 * \sin\tau)}{R_{b1}}\right\} \\ &+ 3(\theta_{b1}-\tau)\tan\tau\sin\tau\left\{\frac{L_1}{R_{b1}} - \cos\theta_{b1} - \cos\tau + (\theta_{b1}-\tau)\sin\tau\right\}^2\Bigg] \end{aligned} \quad (39)$$

$$Q_s(\tau) = 5E_1L[(\theta_{b1}-\tau)\cos\tau + \sin\tau]^3 \quad (40)$$

Hertzian contact stiffness (K_h)

$$\frac{1}{K_h} = \frac{\pi E_1 L}{4(1-\nu_1{}^2)} \quad (41)$$

Effective tooth stiffness (K_e)

$$\frac{1}{K_e} = \frac{1}{K_b} + \frac{1}{K_s} + \frac{1}{K_a} + \frac{1}{K_h} \quad (42)$$

To find stiffness of the corresponding tooth of the gear 2, the subscripts in the above equations are to be changed from 1 to 2. Φ_2 is redefined as

$$\Phi_2 = \frac{X_2}{R_{b2}} - \theta_{b2} \quad (43)$$

$$X_2 = L_p - X_1 \quad (44)$$

$$\theta_{b2} = \frac{\pi}{2Z_2} + \mathrm{inv}(\alpha_0) \quad (45)$$

$$X_1 = R_{b1}(\Phi_1 + \theta_{b1}) \quad (46)$$

Similarly, for the second pair of teeth X_1,X_2, $\Phi_1$and Φ_2 are to be replaced by X_3,X_4, $\Phi_3$and Φ_4 and for the third pair by X_5,X_6, $\Phi_5$and Φ_6 respectively, where

$$X_3 = X_1 + T_0 \quad (47)$$

$$X_4 = L_p - X_3 \quad (48)$$

$$X_5 = X_1 + 2T_0 \quad (49)$$

$$X_6 = L_p - X_5 \quad (50)$$

$$\Phi_3 = \frac{X_3}{R_{b1}} - \theta_{b1} \quad (51)$$

$$\Phi_4 = \frac{X_4}{R_{b2}} - \theta_{b2} \tag{52}$$

$$\Phi_5 = \frac{X_5}{R_{b1}} - \theta_{b1} \tag{53}$$

$$\Phi_6 = \frac{X_6}{R_{b2}} - \theta_{b2} \tag{54}$$

3.2.2 MESH STIFFNESS

The derivation of expression for the mesh stiffness is based on the fact that each meshing pair is modelled as two springs joined in series and thus subjected to same load.

If the stiffnesses of teeth A, B, C, D, E and F are denoted by K_A, K_B, K_C, K_D, K_E and K_F respectively, then the combined stiffness of each meshing pair is

$$K_{p1} = \frac{K_A K_D}{K_A + K_D} \tag{55}$$

$$K_{p2} = \frac{K_B K_E}{K_B + K_E} \tag{56}$$

$$K_{p3} = \frac{K_C K_F}{K_C + K_F} \tag{57}$$

3.3 LOAD SHARING IN PAIRS

To calculate the individual tooth load, the profile modification and tooth error are not considered. When three pairs of teeth are in contact, then

$$F_1 = F \frac{K_{p1}}{K_{p1} + K_{p2} + K_{p3}} \tag{58}$$

$$F_2 = F \frac{K_{p2}}{K_{p1} + K_{p2} + K_{p3}} \tag{59}$$

$$F_3 = F\frac{K_{p3}}{K_{p1}+K_{p2}+K_{p3}} \tag{60}$$

When two pairs are in contact, for example, teeth A and B on the driving teeth remain in contact with teeth D and E on the driven, then

$$K_{p1} = \frac{K_A K_D}{K_A+K_D} \quad \text{and} \quad K_{p2} = \frac{K_B K_E}{K_B+K_E} \tag{61}$$

$$F_1 = F\frac{K_{p1}}{K_{p1}+K_{p2}} \tag{62}$$

$$F_2 = F\frac{K_{p2}}{K_{p1}+K_{p2}} \tag{63}$$

3.4 DYNAMIC LOAD

The dynamic load F_{dj} on the teeth pair is given by following equation

$$F_{dj} = K_{pj}(X_r) + C_{gj}(\dot{X}_r) \tag{64}$$

3.5 CONTACT STRESS ANALYSIS

Contact stresses in contact region can be calculated by using following equations. X axis is considered along the contact width, y axis along contact length and Z axis is perpendicular to the contact surface. Origin of axes is at mid-point of contact area.

$$\sigma_{zz} = \frac{P_0}{\pi}[z(b\Phi_1 - x\Phi_2)] \tag{65}$$

$$\sigma_{xx} = -\frac{P_0}{\pi}\left\{z\left(\frac{b^2+2z^2+2x^2}{b}\Phi_2 - \frac{2\pi}{b} - 3x\Phi_3\right) + \mu[(2x^2 - 2b^2 - 3z^2)\Phi_3] + \frac{2\pi x}{b} + 2(b^2 - x^2 - z^2)\left(\frac{x}{b}\right)\Phi_2\right\} \tag{66}$$

$$\sigma_{yy} = \mu(\sigma_{zz} + \sigma_{xx}) \tag{67}$$

$$\tau_{zx} = -\frac{P_0}{\pi}\left\{z^2\Phi_3 + \mu\left[(b^2 + 2x^2 + 2z^2)\left(\frac{z}{b}\right)\Phi_2\right] - 2\pi\left(\frac{z}{b}\right) - 3xz\Phi_2\right\} \quad (68)$$

Where

$$\Phi_1 = \frac{\pi(M+N)}{MN(2MN+2X^2+2Z^2-2b)^{0.5}} \quad (69)$$

$$\Phi_2 = \frac{\pi(M-N)}{MN(2MN+2X^2+2Z^2-2b)^{0.5}} \quad (70)$$

$$M = [(b+x)^2 + z^2]^{0.5} \quad (71)$$

$$N = [(b-x)^2 + z^2]^{0.5} \quad (72)$$

$$P_0 = \left(\frac{2P}{\pi L\Delta}\right)^{0.5} \quad (73)$$

$$b = \left(\frac{2P\Delta}{\pi L}\right)^{0.5} \quad (74)$$

$$\Delta = 2\rho_R\left(\frac{1-\mu_1^2}{E_1} - \frac{1-\mu_2^2}{E_2}\right) \quad (75)$$

$$\rho_R = \frac{\rho_1\rho_2}{\rho_1+\rho_2} \quad (76)$$

Following equations are used to calculate the stresses on the surface

$$\sigma_{xx} = -2\mu P_o\left[\frac{x}{b} - \left(\frac{x^2}{b^2} - 1\right)^{0.5}\right],\ x \geq b \quad (77)$$

$$\sigma_{xx} = -2\mu P_o\left[\frac{x}{b} + \left(\frac{x^2}{b^2} - 1\right)^{0.5}\right],\ x \leq b \quad (78)$$

$$\sigma_{xx} = -P_o\left[\frac{2\mu x}{b} + \left(1 - \frac{x^2}{b^2}\right)^{0.5}\right],\ -b \leq x \leq b \quad (79)$$

$$\sigma_{zz} = -P_o\left[\left(1-\frac{x^2}{b^2}\right)^{0.5}\right], -b \le x \le b \quad (80)$$

$$\sigma_{zz} = 0,\ x \le -b\ , x \ge b \quad (81)$$

$$\tau_{zx} = -\mu P_o\left[\left(1-\frac{x^2}{b^2}\right)^{0.5}\right],\ x \le -b\ ,x \ge b \quad (82)$$

The principal stresses in the X-Z plane can be calculated by using the equations for principal strain for plain strain condition

$$\sigma_{1,2} = \frac{\sigma_{zz}+\sigma_{xx}}{2} \pm \left[\left(\frac{\sigma_{zz}+\sigma_{xx}}{2}\right)^2 + \tau_{zx}^2\right]^{0.5} \quad (83)$$

$$\sigma_3 = \sigma_{yy} \quad (84)$$

Table 1 Gear data

Item	Driver	Driven
Number of teeth	38	135
Pressure angle(^{0})	17.5	17.5
Module (mm)	2.674	2.674
Pitch diameter(mm)	101.6	360.946
Contact ratio	2.24	2.24
Face width (mm)	73.66	73.66
Root diameter(mm)	94.6125	351.7417
Form diameter(mm)	97.5182	354.5027
Outside diameter(mm)	109.3521	366.1207
Pitch circular thickness (mm)	3.9497	9.9827
Steady transmitted load(KN)	30	30
E (For steel) (GPa)	210	210

CHAPTER 4

RESULT AND DISSCUSSION

4.1 MESH STIFFNESS

For the gear drive with standard proportions, the dimensions and properties are given in Table 1 while the variation of tooth stiffness along the path of contact for the driving gear and driven gear are shown in Figure 4.1. The variation of mesh stiffness along the path of contact is also shown in same figure. It has been observed that stiffness of the driving gear tooth decreases, whereas the stiffness of the driven gear tooth increases along the path of contact. This is due to the fact that on the driving gear, the contact point moves from root to the tip of the tooth whereas on the driven gear, the contact point moves from tip to the root. In general tooth is more flexible at the outside than it is near the root.

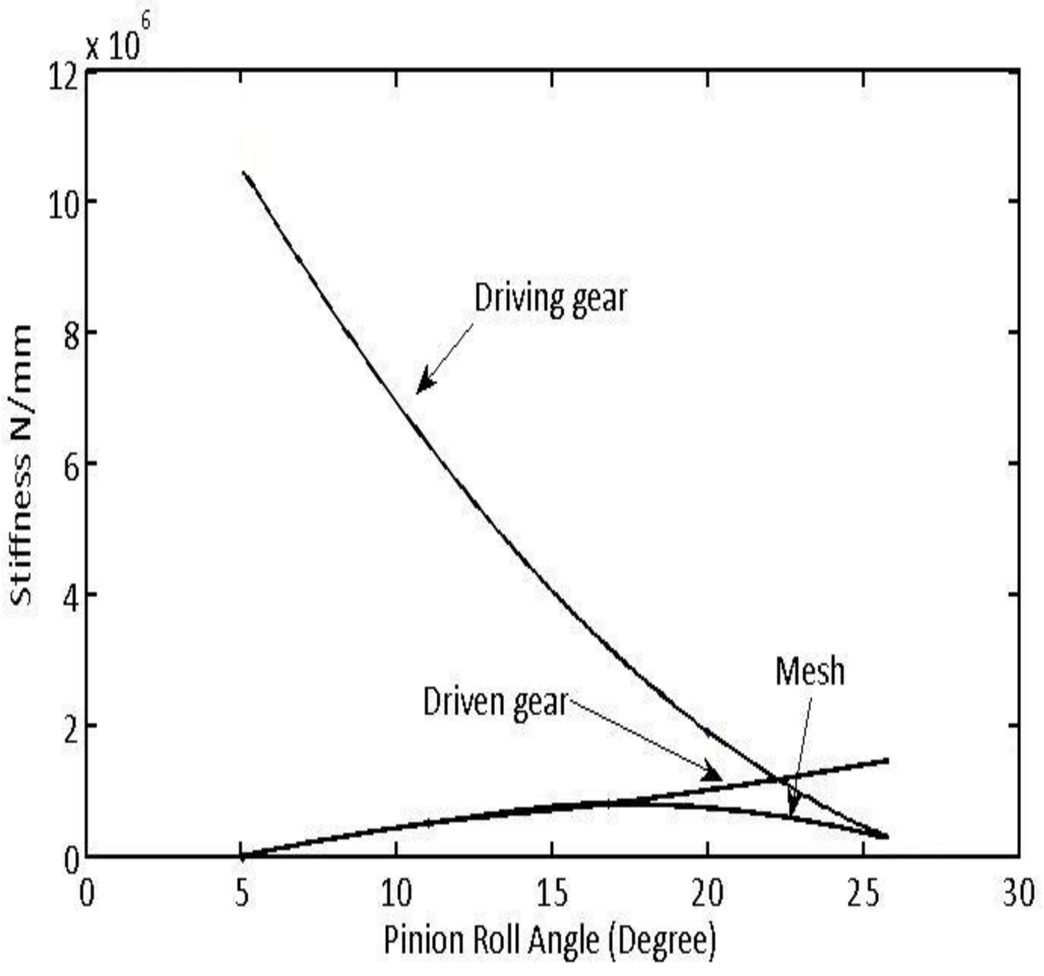

Figure 4.1 Stiffness variations with pinion roll angle

4.2 NORMAL TOOTH LOAD

The variation of individual tooth normal load along the path of contact for various pinion roll angles is shown in Figure 4.2. This shows that the normal load reaches its maximum in the two pairs contact zone.

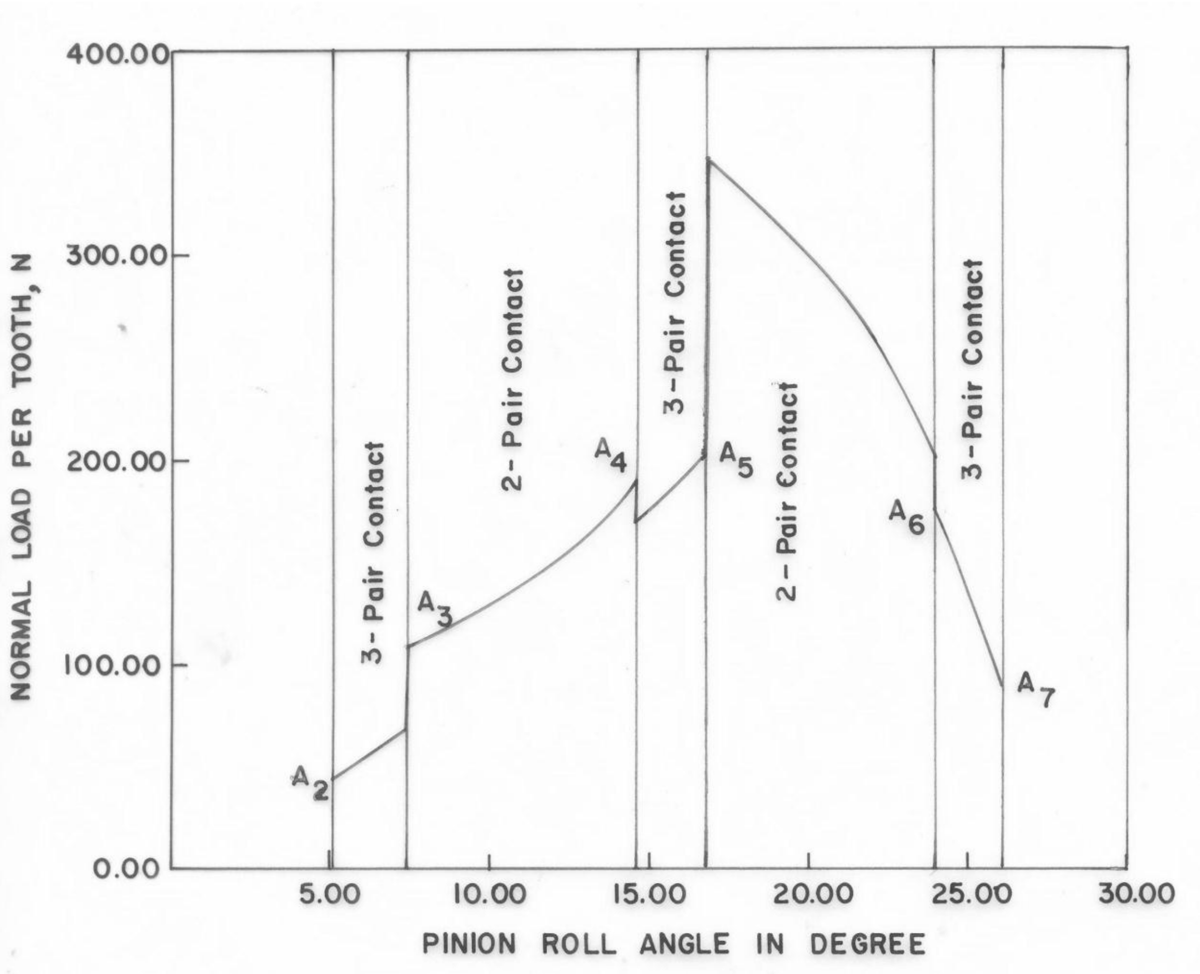

Figure 4.2 Tooth Load sharing

As shown in Figure 4.2, normal load per tooth is high in the regions of two pairs contact while load is low in the regions of three pairs in contact. It is due to the load sharing between teeth pairs. In the region where pinion roll angle varies from 16.783^0 to 23.998^0, normal load per tooth is having highest value and it decreases when it approaches to the region of three pairs in contact.

4.3 DYNAMIC LOAD

It is observed that the dynamic loads acting on the gear tooth is very much affected by the operating speed. At pinion speed of 1 rpm, two pairs and three pairs contact regions and transition between them can be distinguished clearly. At very low speeds the instantaneous load acting on the gear tooth is same as steady transmitted load.

Refer Figure 4.3

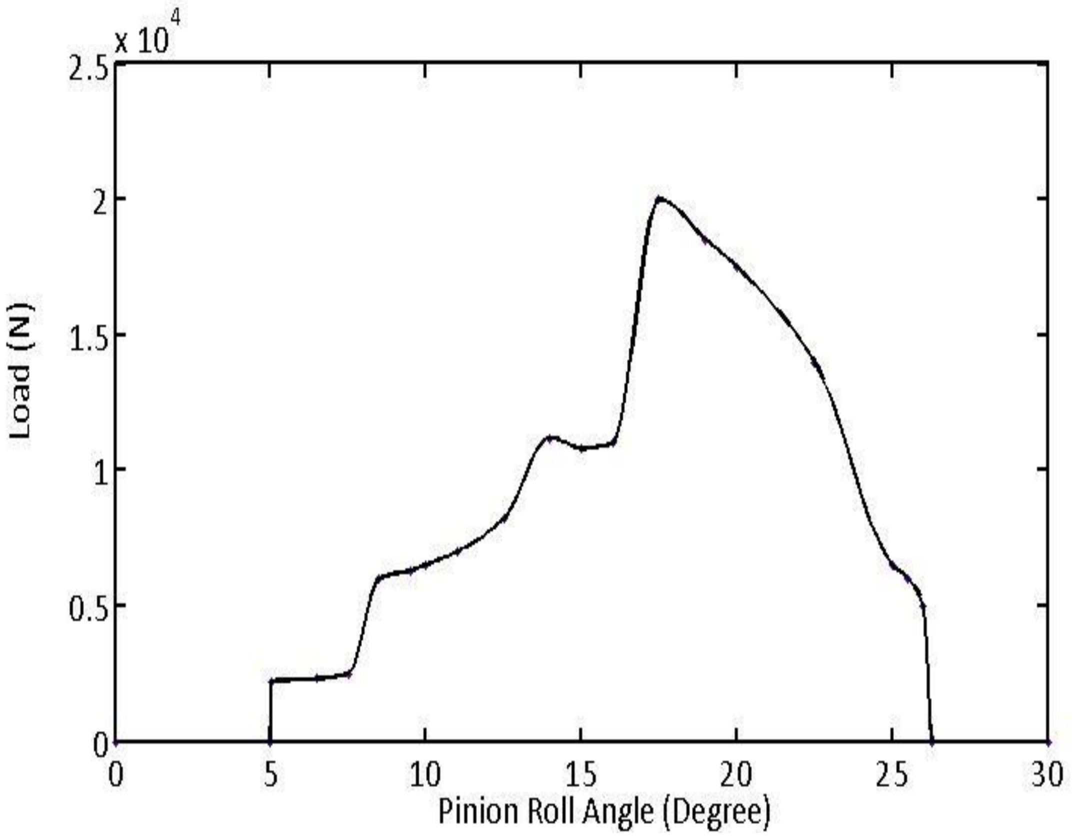

Figure 4.3 Variation of dynamic load on the pinion tooth for 1 rpm pinion speed

For pinion roll angles of 5.038^0 to 7.312^0, 14.512^0 to 16.785^0 and 23.988^0 to 26.258^0, there are three pairs in contact.

For pinion angles of 7.312^0 to 14.512^0 and 16.785^0 to 23.988^0, there are two pairs in contact.

Dynamic load variations for different operational speed are shown in the Figure 4.4, 4.5 and 4.6

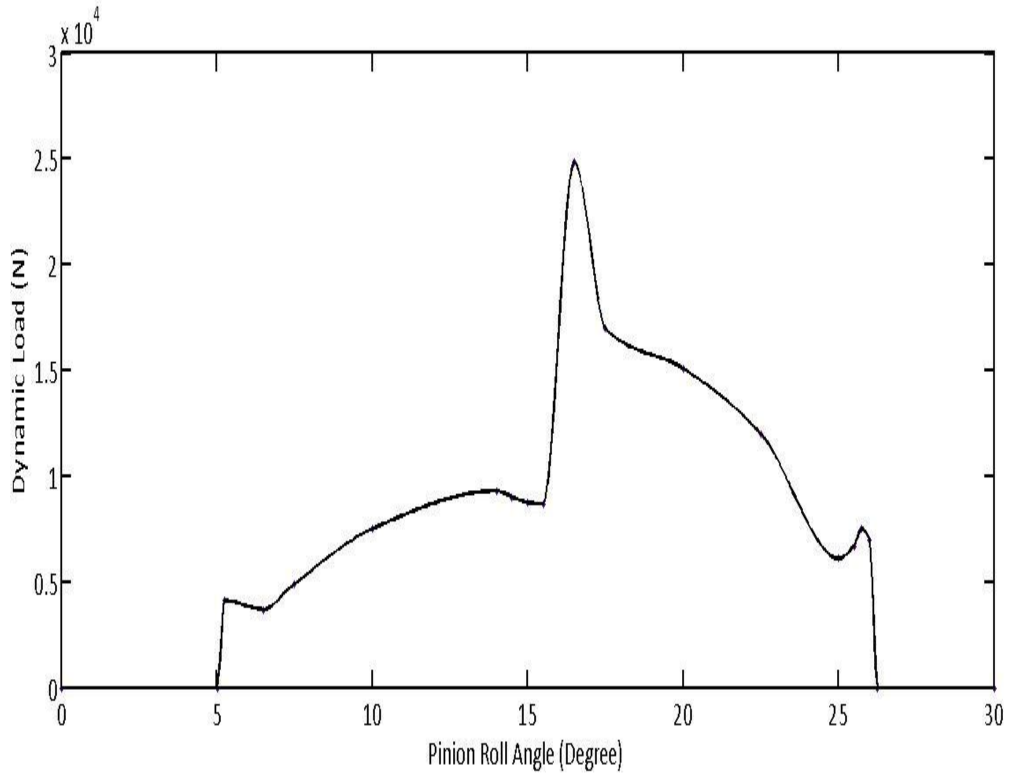

Figure 4.4 Variation of dynamic load on pinion tooth for 2500 rpm

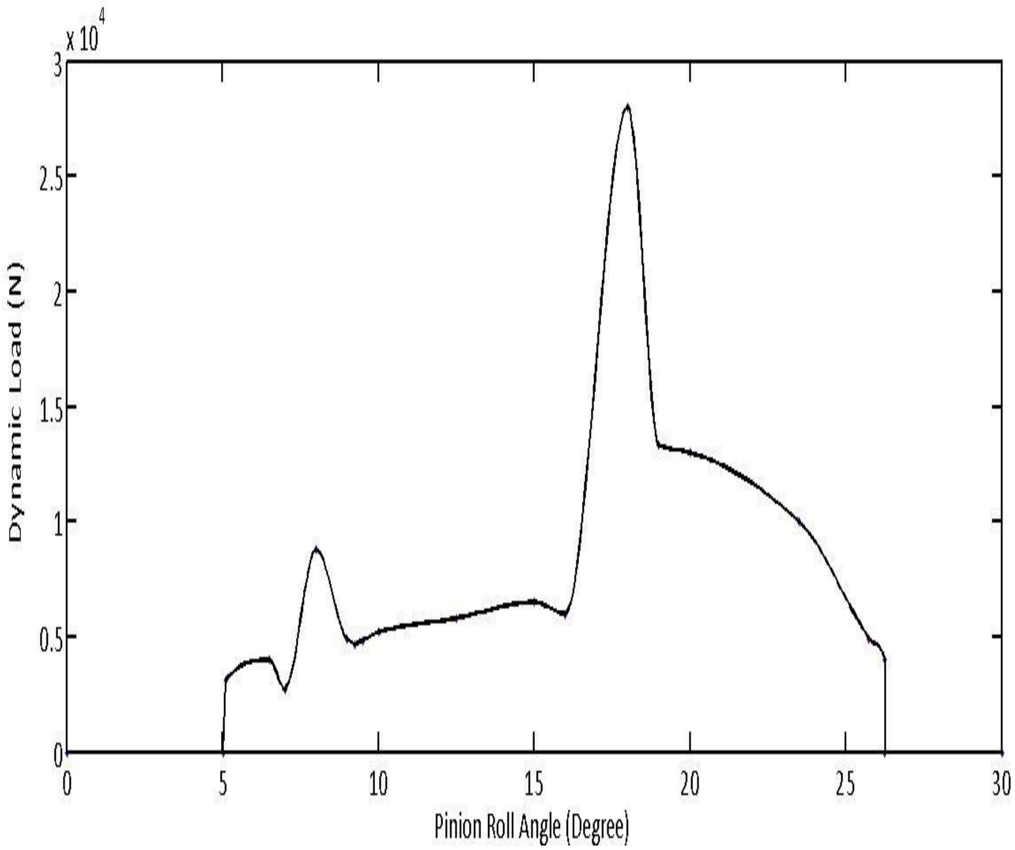

Figure 4.5 Variation of dynamic load on pinion tooth for 5000 rpm

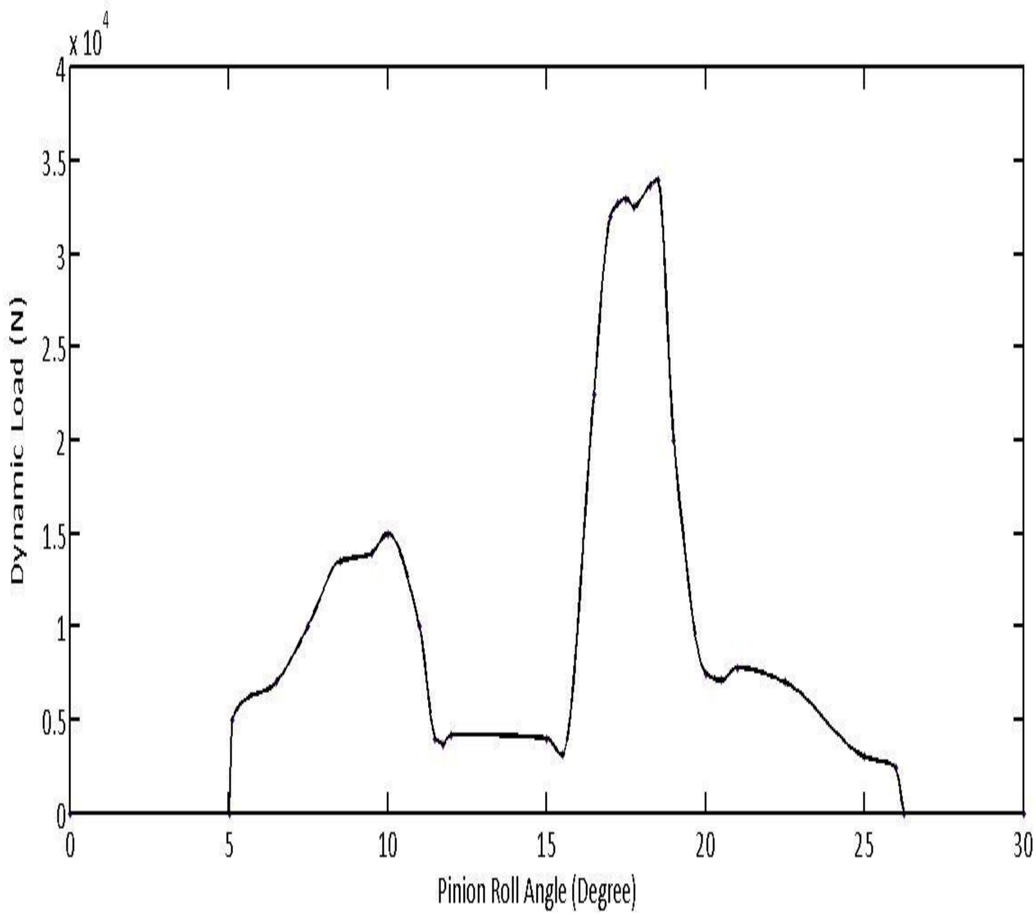

Figure 4.6 Variation of dynamic load on pinion tooth for 10000 rpm

At speeds like 2500, 5000 and 10000 rpm; mesh stiffness varies along pinion roll angle hence dynamic load fluctuates. Such fluctuations are large when there is transition from three pairs contact regions and vice versa. Due to change in number of pairs in contact, the value of effective mesh stiffness changes in large amount. Maximum change of effective stiffness occurs at second change of three pairs contact region to two pairs contact region (pinion roll angle 16.785^0) hence the maximum dynamic load is observed at this transition point. The maximum value of dynamic load increases with increase in operational speed because of increased rate of change of mesh stiffness along with operational speed. As operational speed increases the location of maximum dynamic load shifts to higher pinion roll angle.

4.4CONTACT STRESSES

Variation of contact stresses depends on variation of dynamic loads. At very low operating speeds the contact stresses vary in the same pattern as that of static loading. At speeds like 2500, 5000 and 10000 rpm; dynamic load varies along pinion roll angle hence contact stress fluctuates prominently.

In the following figures contact stresses variations for different operational speed are shown

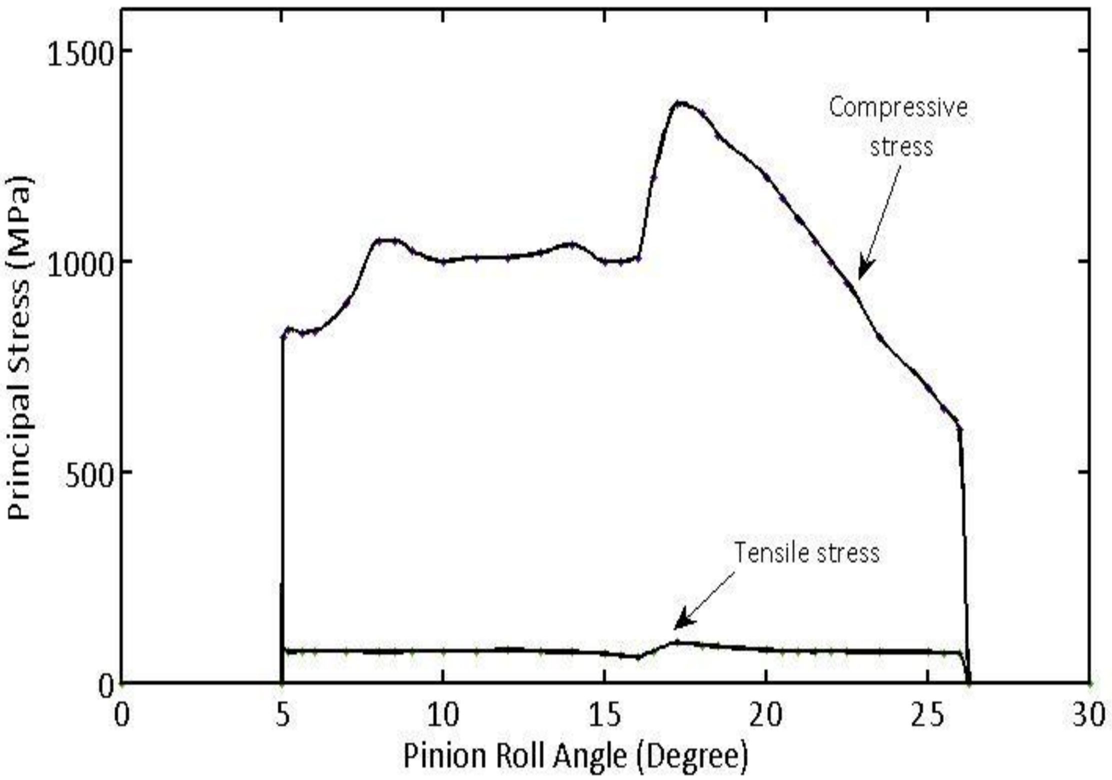

Figure 4.7 Variation of compressive and tensile principal stresses on pinion tooth for 1 rpm

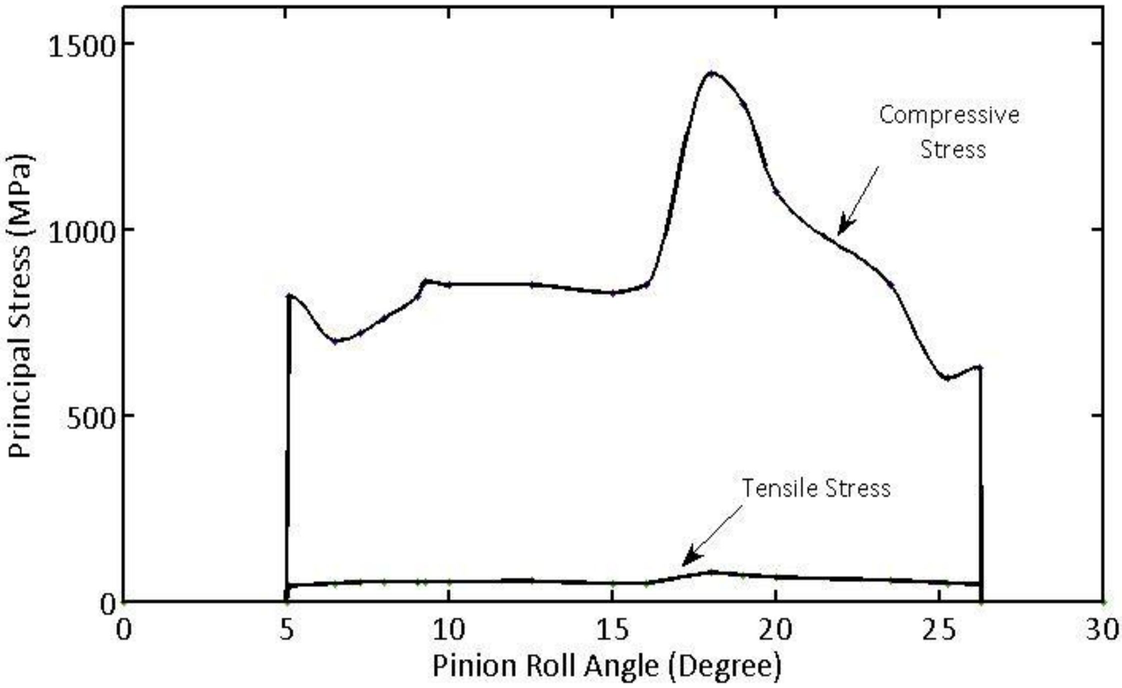

Figure 4.8 Variation of compressive and tensile principal stresses on pinion tooth for 2500 rpm

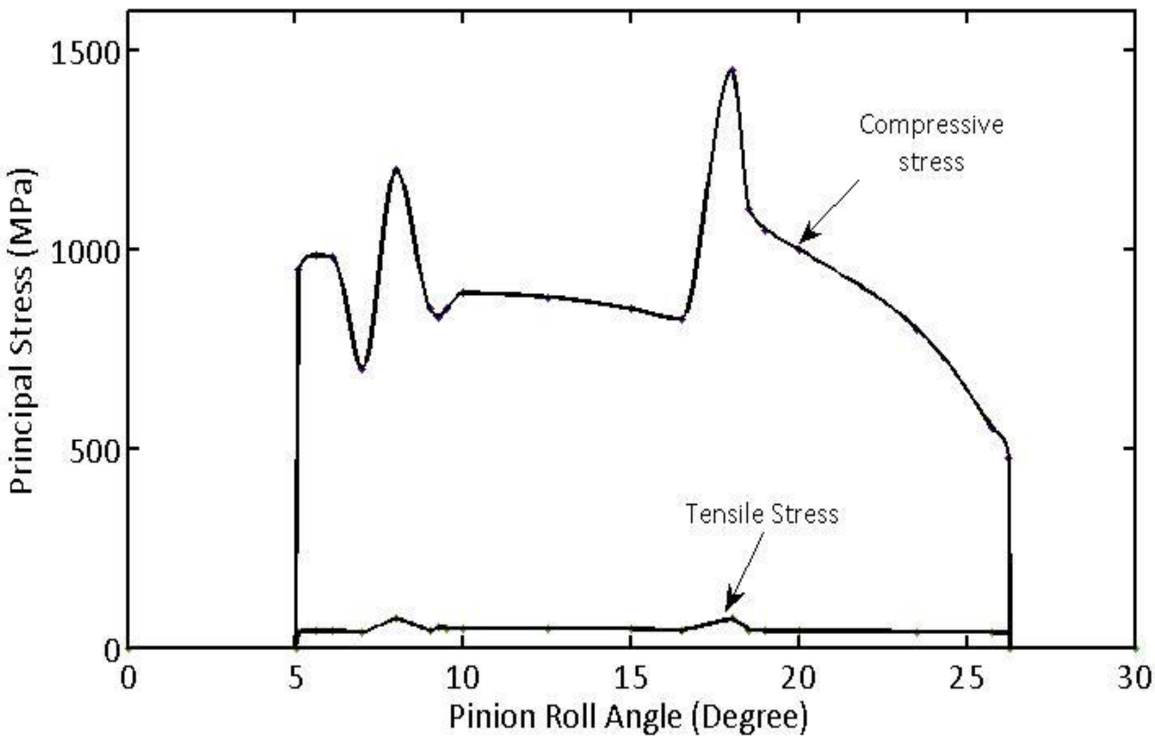

Figure 4.9 Variation of compressive and tensile principal stresses on pinion tooth for 5000 rpm

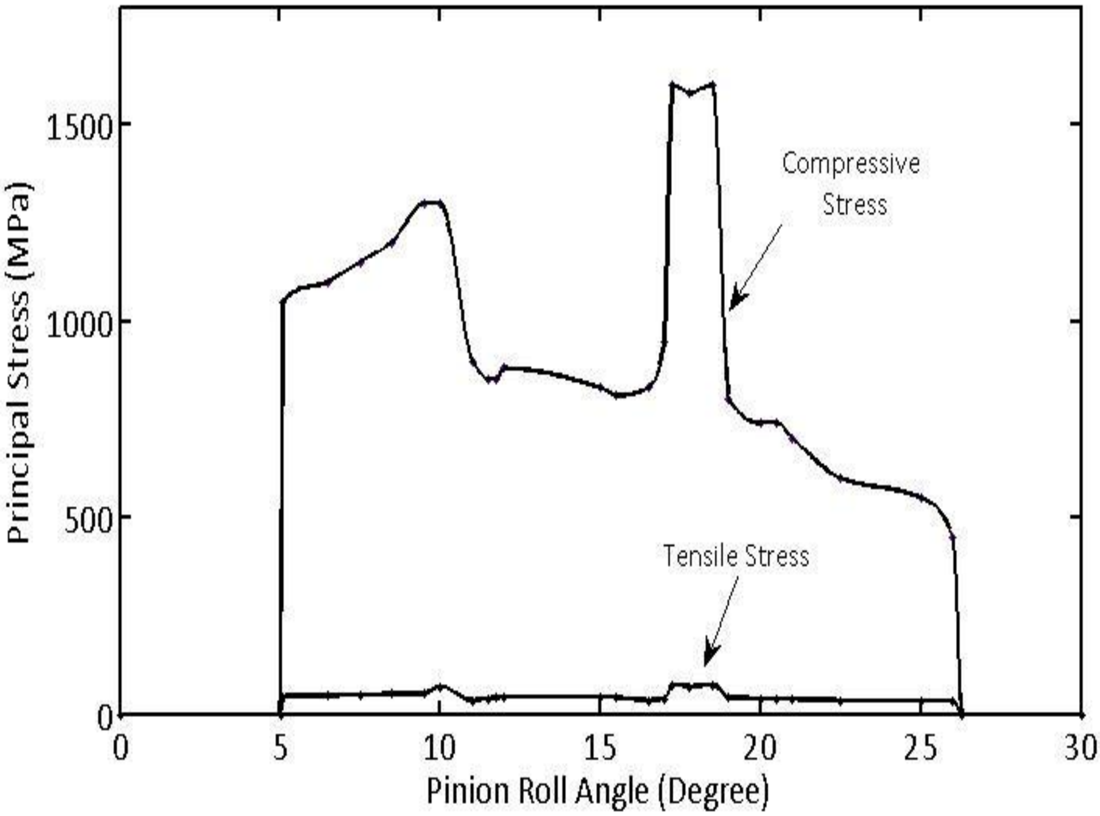

Figure 4.10 Variation of compressive and tensile principal stresses
on pinion tooth for 5000 rpm

From the above figures, it is observed that the principal stresses increase with increase in operational speed. At 10000 rpm pinion speed; principal stresses are very high. Stresses vary in the same pattern as that of dynamic load. Principal stresses are high in the two pairs of contact region than that of three pair contact region. Principal stresses are having higher value in the region where pinion roll angle changes from 16.783^0 to 23.988^0. Compressive stresses are dominant than tensile stresses.

CHAPTER 5

CONCLUSION & FUTURE SCOPE

5.1 CONCLUSION

The present work gives an analytical method for calculation of the tooth load sharing in high contact ratio spur gear pairs at any point in mesh cycle. It also gives the stiffness variation of driving gear, driven gear and mesh with respect to pinion roll angle. For dynamic load analysis of high contact ratio spur gear system, a torsional vibration based model is used. This gives the effect of operational speed on magnitude of dynamic load acting on pinion tooth also on the principal stresses acting on pinion tooth. Effect of operational speed on the location of maximum dynamic load is predicted here.

From the foregoing discussion it is concluded that

- Stiffness of the driving gear tooth decreases along the path of contact whereas the stiffness of the driven gear tooth increases along the path of contact. In general tooth is more flexible at the outside than it is near the root.
- Normal load acting on pinion tooth has maximum value in the two pairs contact region.
- At low speed, the instantaneous load acting on pinion tooth is same as that of static transmitted load.
- Due to change in effective stiffness in second change of three pairs contact zone to two pair of contact zone, maximum dynamic load and principal stresses are observed in this region.
- Variation of operational speed has an influence on the magnitude of dynamic load acting on pinion tooth
- Location of maximum dynamic load acting on pinion tooth is very much affected by operational speed.

5.2 FUTURE SCOPE

- This study can be carried out further including the flexibility of disks, shafts on which gears are mounted and bearings.
- This method of analysis can be applied to other forms of tooth profile like cycloid, non-involute, non-standard etc. with the proper modification.
- This analysis can be extended for other type of gears with composite materials.
- Two dimensional and Three Dimensional contact analysis can be done using ANSYS and then compared with the analytical results.

CHAPTER 6

REFERENCES

6 REFERENCES

[1] W. A. Tuplin, "Gear Tooth Stresses at High Speed", Proceedings of the Institution of Mechanical Engineers, 1950, Vol. 163, page 162-175.

[2] J. O. Smith and C. K. Liu, "Stresses due to Tangential and Normal Loads on an Elastic Solid with Application to some Contact Stress Problems", Journal of Applied Mechanics, 1953, Vol. 20, page 157.

[3] D. R. Houser and A. Seireg, "Evaluation of Dynamic Factors for Spur and Helical Gears", ASME J. Eng. Ind. , 1970, Vol. 92, page 504–514.

[4] L. Wilcox and W. Coleman, "Application of Finite Elements to the Analysis of Gear Tooth Stresses", Journal of Manufacturing Science Engineering, 1973, Vol. 95, Issue 4, page1139-1148.

[5] H.E.Staph, "A Parametric Analysis of High Contact Ratio Spur Gears", ASLE Transections, 1976, Vol.19, Issue 3, page 201-215.

[6] R. W. Cornell and W. W. Westervelt, "Dynamic Tooth Loads and Stressing for High Contact Ratio Spur Gears", Journal of Mechanical Design, 1978, Vol. 100, Issue 1, page 69-76.

[7] J.W. Lund, "Critical Speeds, Stability and Response of a Geared Train of Rotors", ASME Journal of Mechanical Design, 1978, Vol.100, page 535-538.

[8] R. Kasuba and J. W. Evans, "An Extended Model for Dynamic Loads in Spur Gearing", ASME Journal of Mechanical Design, 1981, page 398-409.

[9] A. H. Elkholy, "Tooth Load Sharing in High-Contact Ratio Spur Gears", Journal of Mechanical Design, 1985, Vol. 107, Issue1, page11-16.

[10] D. C. Yang and J. Y. Lin, “Hertzian Damping, Tooth Friction and Bending Elasticity in Gear Impact Dynamics”, ASME Journal of Mechanisms, Transmissions and Automation in Design, 1987, Vol. 109, page 107.

[11] H. Nevzat Ozguven and D. R. Houser, “Dynamic Analysis of High Speed Gears using Loaded Static Transmission Error”, Journal of Sound and Vibration, 1988, Vol. 125, Issue1, page 71-83.

[12] A. Kahraman and R. Singh “Error Associated With a Reduced Order Linear Model of a Spur Gear Pair”, Journal of Sound and Vibration, 1991, Vol. 149, Issue 3, page 495-498.

[13] A. Kahraman, H. N. Ozguven and D. R. Houser, “Dynamic Analysis of Geared Rotor by Finite Element”, ASME Journal of Mechanical Design, 1992, Vol. 114, Issue 2, page 507-514.

[14] S. K. Nayak, “Effect of Tooth Stiffness on Dynamic Load on Spur Gear Teeth in Mesh”, ME Thesis Regional Engineering College, Rourkela, Odisha, 1994.

[15] V. Ramamurti, H. Nayak, Vijayendra and C. Sujatha “Static and Dynamic Analysis of Spur and Bevel Gears using FEM”, Mechanical Machine Theory, 1998, Vol. 33, Issue 8, page 1177-1193.

[16] R. G. Parker, S. M. Vijayakar and T. Imajo, “Non-Linear Dynamic Response of a Spur Gear Pair: Modelling and Experimental Comparisons”, Journal of Sound and Vibration, 2000, Vol. 237, Issue 3, page 435-455.

[17] K. J. Huang and T. S. Liu,“Dynamic Analysis of Spur Gear by Dynamic Stiffness Method”, Journal of Sound and vibration, 2000, Vol. 234, Issue 2, page 311-329.

[18] A.Kapelevich, “Geometry and design of involute spur gears with asymmetric teeth”, Mechanism and Machine Theory, 2000, Vol.135, page 117-130.

[19] Siu-Tong Choi and Sheng-Yang Mau, “Dynamic Analysis of Geared Rotor-Bearing Systems by the Transfer Matrix Method”, Journal of Mechanical Design, 2001, Vol. 123, page 562-568.

[20] Zhang Hua Fong, Ta Wei Chiang and Chieh Wen Tsey, “Mathematical Model for Parametric Tooth Profile of Spur Gear Using Line of Action”, Mathematical and Computer Modeling, 2002, Vol. 36, page 603-614.

[21] L. Vedmar and A. Anderson, “A Method to Determine Dynamic Loads on Spur Gear Teeth and on Bearings”, Journal of Sound and Vibration, 2003, Vol. 267, page 1065–1084.

[22] Rafiq Maliha, Can U. Dogruer and H. Nevzatozguven, “Nonlinear Dynamic Modeling of Gear Shaft Disk Bearing Systems Using Finite Elements and Describing Functions”, Transactions of the ASME, 2004, Vol. 126, page 534-541.

[23] Jiande Wang and Ian Howard, “Finite Element Analysis of High Contact Ratio Spur Gears in Mesh”, Journal of Tribology, 2005, Vol. 127, page 469-483.

[24] Shuting Li, “Finite Element Analysis for Contact Strength and Bending Strength of A Pair of Spur Gears With Machining Errors, Assembly Errors And Tooth Modifications”, Mechanism and Machine Theory, 2007, Vol.42, page 88–114.

[25] E. Podzharov, V. Syromyatnikov, J. Navarro and R. Navarro, “Static and Dynamic Transmission Error in Spur Gears”, The Open Industrial and Manufacturing Engineering Journal, 2008, Vol. 1, page 37-41.

[26] Shuting Li, “Effect of Addendum on Contact Strength, Bending Strength and Basic Performance Parameters of a Pair of Spur Gears”, Mechanism and Machine Theory, 2008,Vol. 43, page 1557–1584.

[27] F. Karpat, S. E. Osire, K. Cavdar and F. C.Babalik, “Dynamic Analysis of Involute Spur Gears with Asymmetric Teeth”, International Journal of Mechanical Sciences, 2008, Vol.50, page 1598–1610.

[28] W. Kim, H. H. Yoo and J. Chung, “Dynamic Analysis for a Pair of Spur Gears with Translational Motion due to Bearing Deformation”, Journal of Sound and Vibration, 2010, Vol. 329, page 4409–4421.

[29] M. Ristivojevic, T. Lazovic and A. Vencl, “Studying the Load Carrying Capacity of Spur Gear Tooth Flanks”, Mechanism and Machine Theory, 2013, Vol.59, page 125–137.

[30] A. F. Rincon, F. Viadero , M. Iglesias, P. Garcia, A. de-Juan and R. Sancibrian, “A Model for the Study of Meshing Stiffness in Spur Gear Transmissions”, Mechanism and Machine Theory, 2013, vol. 61, page 30–58.